General Disclaimer

One or more of the Following Statements may affect this Document

- This document has been reproduced from the best copy furnished by the organizational source. It is being released in the interest of making available as much information as possible.

- This document may contain data, which exceeds the sheet parameters. It was furnished in this condition by the organizational source and is the best copy available.

- This document may contain tone-on-tone or color graphs, charts and/or pictures, which have been reproduced in black and white.

- This document is paginated as submitted by the original source.

- Portions of this document are not fully legible due to the historical nature of some of the material. However, it is the best reproduction available from the original submission.

Produced by the NASA Center for Aerospace Information (CASI)

MASTER

ORNL/TM-5480

Surface Tension Induced Convection in Encapsulated Liquid Metals in Microgravity—Apollo-Soyuz Test Project Experiment No. MA-041

R. E. Reed
H. L. Adair
W. Uelhoff

OAK RIDGE NATIONAL LABORATORY

ORNL/TM-5480

Contract No. W-7405-eng-26

Solid State Division

SURFACE TENSION INDUCED CONVECTION IN ENCAPSULATED LIQUID METALS IN MICROGRAVITY - APOLLO-SOYUZ TEST PROJECT EXPERIMENT NO. MA-041

R. E. Reed,[†] H. L. Adair, and W. Uelhoff[*]

[†]Deceased.

[*]Guest scientist from Institut für Festkörperforschung, Kernforschungsanlage Jülich, BRD.

Date Published: December 1976

TABLE OF CONTENTS

SURFACE TENSION INDUCED CONVECTION IN ENCAPSULATED LIQUID METALS IN MICROGRAVITY – APOLLO-SOYUZ TEST PROJECT EXPERIMENT NO. MA-041

R. E. Reed, H. L. Adair, and W. Uelhoff

ABSTRACT

One objective of the Apollo-Soyuz Test Project (ASTP) was to conduct scientific experiments in a gravity-free environment to permit the study of melting and solidification processes as well as liquid processes in space. It has been shown by Skylab experiments that surface driven convection caused by temperature gradients (Marangoni effect) is negligibly small. This experiment was designed to determine the extent of surface tension induced convection caused by a steplike compositional variation in a liquid metal.

This report describes preliminary results obtained for ASTP Experiment No. MA-041 entitled "Surface Tension Induced Convection in Encapsulated Liquid Metal in Microgravity."

INTRODUCTION

The purpose of this investigation was to set up a liquid diffusion couple of lead (Pb) and Pb-0.05 atomic percent (at. %) gold (Au) alloy in a microgravity environment. The liquid diffusion couple was contained in two types of ampoules, a 1015 steel container that the liquid metal would wet and an LTJ graphite container that the liquid metal would not wet. The couples were to be in the molten state for a reasonable time compared to the available diffusion length of 3 cm. If there were no convective stirring effects due to the surface tension differences between the Pb and Pb-0.05 at. % Au alloy, then a normal concentration-distance profile for the Au could be found in the diffusion couples.

Because there were two diffusion temperatures 923 and 743 K (650°C and 470°C), the liquid diffusion parameters for Au in Pb can be estimated. If there were convective stirring effects due to the surface tension variations caused by the Au additions, then these could also be found by the autoradiographic technique used for the diffusion analysis. The wetting and nonwetting ampoules can be examined to evaluate the extent of the stirring effects.

EXPERIMENT DESIGN

The general concept of the experiment, specimen ampoule preparation, and experimental design can be found in references 1, 2. However, a brief description of the experimental design will help to clarify the results obtained. A schematic representation showing the arrangement of the specimens in the multipurpose electric furnace is shown in Fig. 1. Because of longitudinal heat flow in the furnace upon heating and cooling, the specimens melted from left to right with reference to the representation, Fig. 1, and solidified in the reverse direction; as is shown, a total of six specimens were used in the experiment aboard Apollo-Soyuz. The furnace and the cartridges which contained the specimen ampoules were constructed such that each ampoule would experience minimum temperature gradients. Two of the three flight cartridges contained specimens loaded in graphite containers. The two cartridges were identical except for the fact the Pb and 0.05 at. % Au alloy in one cartridge (Flight Cartridge 2) was located on the end which melted first; in the other cartridge (Flight Cartridge 3) the alloy was located on the reverse end of the specimen and thus melted last and solidified first. This arrangement was done to determine if there was a melting or solidification effect on the Au concentration profile. Flight Cartridge 1 (Fig. 1) contained two specimens in a steel capsule with the Pb-Au alloy aligned such that it melted first. An identical specimen arrangement to the one just described was used for ground base tests to provide comparison between the different transport mechanisms in liquid metals processed in space and in a unit gravity environment.

ORNL-DWG 74-8080
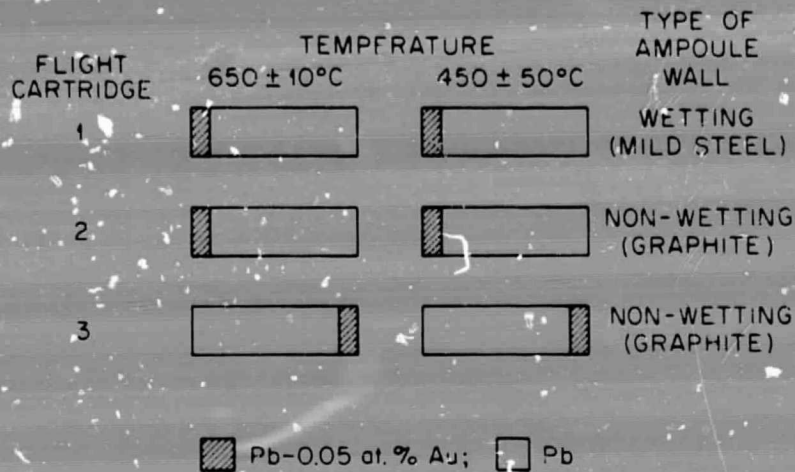
Figure 1. Schematic Arrangement of Specimens

Dimensions of the actual specimens are shown in Fig. 2. The total specimen length was approximately 3 cm and the diameter was approximately 1 cm. The 3-millimeter thick Pb-0.05 at. % Au alloy disk was cold-pressure welded to the pure Pb. It should be noted that the total diffusion distance available was approximately 3 cm.

ORNL-DWG 74-8076R
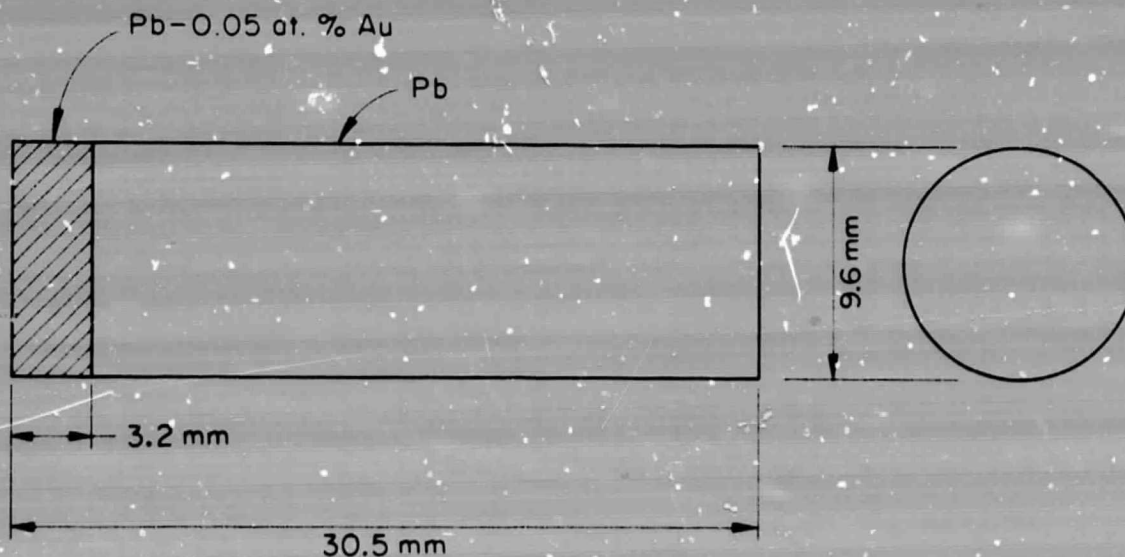
Figure 2. Dimensions of MA-041 Specimen

Ampoules (mild steel and stainless steel lined with graphite) used for the specimens described in this report are shown in Figs. 3 and 4, respectively. In the graphite lined container, quartz cloth disks were placed at each end to provide some padding for normal handling movements and to adjust the void space in the ampoule.

ORNL-DWG 74-8079R
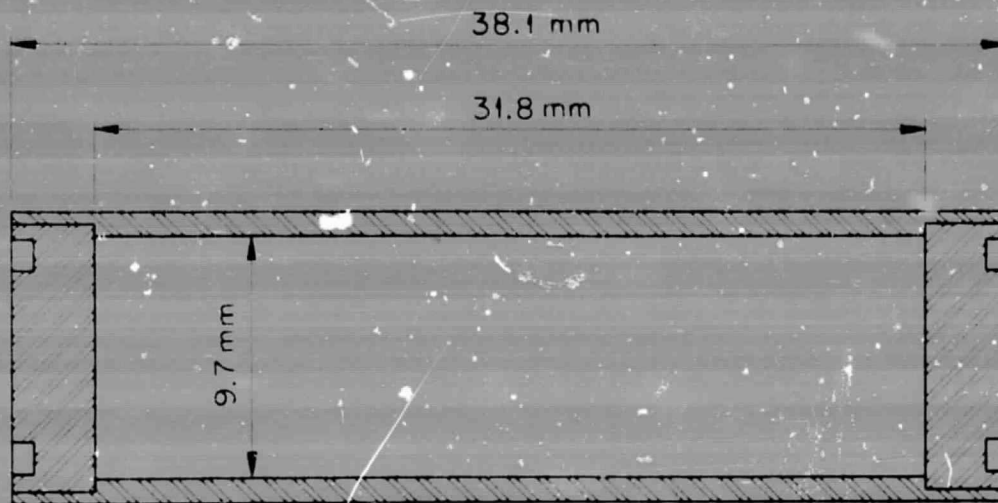
Figure 3. Ampoule assembly constructed of 1015 steel for B type specimen capsules.

ORNL-DWG 74-8078R
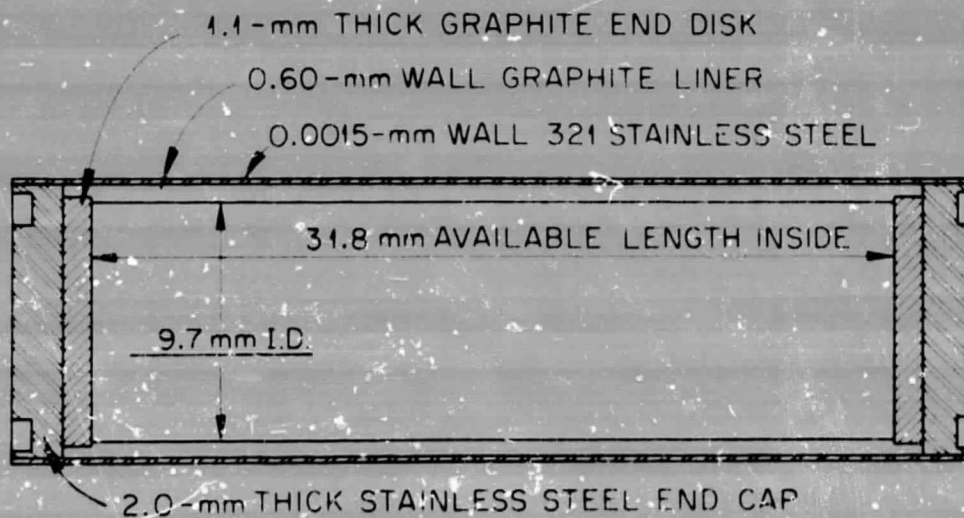
Figure 4. Stainless Steel – Graphite ampoule assembly for A and A-R type specimen capsules.

GROUND BASE AND SPACE FLIGHT THERMAL CHARACTERISTICS OF THE MULTIPURPOSE ELECTRIC FURNACE

Temperature-time data monitored on the mission was obtained by measurements made on the heat-leveler block of the multipurpose furnace. Subsequent to flight, a ground base test was made in which the space flight furnace operation was duplicated since its operation during the actual experiment was different from that originally planned. The thermal characterization analyses to obtain the temperature-time history for the specimen ampoules (both space flight and ground base samples) were made by Teledyne Brown Engineering and the results are shown in Tables 1 through 4.[3] Relative node locations described in Tables 1 through 4 are shown in Fig. 5. Table 5 lists the heating and cooling rates for both ground base and space flight specimens at 600°K; these rates are based on the slopes of the temperature curves for nodes 312 and 322 (Fig. 5). The approximate solidification rates for both the ground base and space flight samples were determined by dividing the change in temperature per unit time by the change in temperature per unit length. The results are shown below:

1. 2.5 cm/min. for the hot zone ground base samples
2. 9.0 cm/min. for the cold zone ground base samples
3. 2.5 cm/min. for the hot zone space flight samples
4. 6.0 cm/min. for the cold zone space flight samples.

It was determined from the flight analyses that the ampoules A and B (Fig. 5) were in the liquid phase for 268 and 82 min., respectively. In the GBT-25 experiment the sample liquid phase duration was 226 and 77 min. for ampoules A and B, respectively.[3]

Table 1. Ampoule A Temperature Profile and Gradient at Selected
Times in GBT-25

Experiment Event	Temperature K					Ampoule Gradient* (K/cm)
	Node 41_	Node	Node 312	Node 313	Node 414	
Pre-Melt	604._	_99.1		598.7	598.4	1.7
Start Soak**			810.3	809.6	809.2	2.0
Mid Soak	925._			921.3	921.0	1.2
End Soak*** (ES)	928.5	9_		924.4	924.1	1.1
ES + 10 min.	899.2	897_	_96.9	896.3	895.9	0.9
ES + 30 min.	827.8	825.9	825.6	825.1	824.9	0.8
ES + 60 min.	739.2	737.8	737.4	737.1	736.9	0.6
Pre-Solidification	603.8	602.8	602.7	602.4	602.3	0.4

*Ampoule gradient = (T 410 − T 414)/3.81.

**Soak started 70 min. after furnace on.

***Soak ended 115 min. after furnace on.

Table 2. Ampoule B Temperature Profile and Gradient at Selected
Times in GBT-25

Experiment Event	Temperature K					Ampoule Gradient* (K/cm)
	Node 420	Node 321	Node 322	Node 323	Node 421	
Start Soak**	545.2	545.1	542.3	540.1	540.1	1.3
Pre-Melt	599.9	599.8	596.8	594.2	594.1	1.5
Mid Soak	691.4	691.2	687.7	684.7	684.6	1.8
End Soak*** (ES)	700.7	700.5	697.0	694.1	693.9	1.8
ES + 10 min.	657.9	657.8	654.3	651.4	651.3	1.7
ES + 30 min.	650.4	650.3	647.7	645.5	645.4	1.3
Pre-Solidification	605.2	605.1	602.6	600.8	600.4	1.3
ES + 60 min.	600.5	600.4	598.2	596.4	596.3	1.1

*Ampoule gradient = (T 410 − T 414)/3.81.

**Soak started 70 min. after furnace on.

***Soak ended 115 min. after furnace on.

Table 3. Ampoule A Temperature Profile and Gradient at Selected
Times in Flight

Experiment Event	Temperature K					Ampoule Gradient* (K/cm)
	Node 410	Node 311	Node 312	Node 313	Node 414	
Pre-Melt	600.6	595.4	594.8	594.7	594.5	1.6
Start Soak**	922.3	919.7	919.2	918.6	918.3	1.1
Mid Soak	932.7	930.3	929.8	929.2	928.9	1.0
End Soak*** (ES)	936.1	933.8	933.3	932.8	932.5	0.9
ES + 10 min.	886.0	884.0	883.5	883.0	882.7	0.9
ES + 30 min.	840.3	839.7	839.3	838.8	838.6	0.5
ES + 60 min.	718.9	717.5	717.2	716.9	716.8	0.6
Pre-Solidification	604.6	603.7	603.5	603.3	603.2	0.4

* Ampoule gradient = (T 410 - T 414)/3.81.

** Start soak 95 min. after furnace on.

*** End soak 127 min. after furnace on.

Table 4. Ampoule A Temperature Profile and Gradient at Selected
Times in Flight

Experiment Event	Temperature K					Ampoule Gradient* (K/cm)
	Node 420	Node 321	Node 322	Node 323	Node 421	
Pre-Melt	597.3	597.2	594.4	592.0	591.9	1.4
Start Soak**	675.1	674.9	671.3	668.2	668.1	1.8
Mid Soak	701.3	701.1	697.5	694.5	694.4	1.8
End Soak*** (ES)	710.7	710.5	707.1	704.1	704.0	1.8
ES + 10 min.	650.2	650.0	646.7	643.8	643.7	1.7
ES + 30 min.	631.3	631.2	628.5	625.8	625.7	1.5
Pre-Solidification	603.5	603.4	601.5	600.6	600.1	0.9
ES + 60 min.	582.7	582.7	581.0	579.5	579.5	0.8

* Ampoule gradient = (T 420 - T 421)/3.81.

** Start soak 95 min. after furnace on.

*** End soak 127 min. after furnace on.

ORNL-DWG 76-5306
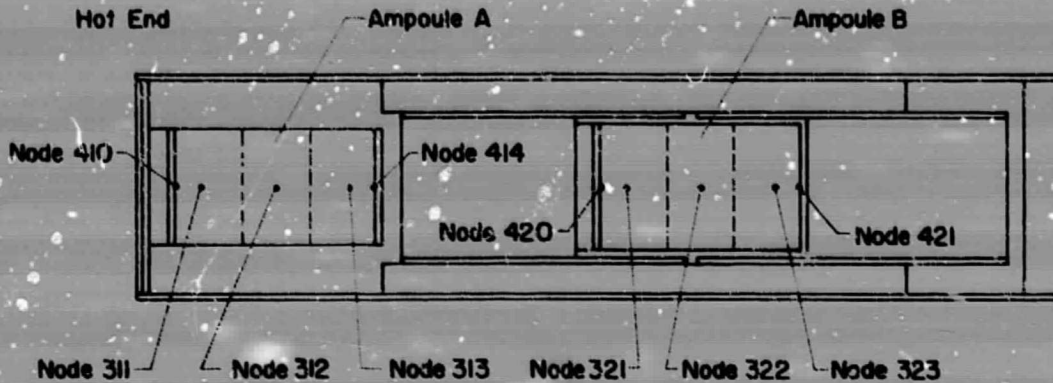
Figure 5. Schematic showing the relative node locations used in both ground base and space flight thermal analyses. Ampoules A and B represent the hot and cold zones of the multipurpose electric furnace, respectively.

Table 5. Heating and Cooling Rates for Ground Base and Space Flight Specimen Ampoules

Characteristic	Ground Base Temperature History[*] (GBT-25 - Teledyne Brown Engineering)		Space Flight Temperature History[**] (Teledyne Brown Engineering)	
	Hot Zone	Cold Zone	Hot Zone	Cold Zone
Heating Rate at 600 K (K/min.)	7	2	11	4
Cooling Rate at 600 K (K/min.)	1	10	1	5

[*]Heating and cooling rates based on the slopes of the temperature curves at 600 K at nodes 312 and 322 for GBT-25.[3]

[**]Heating and cooling rates based on the slopes of the temperature curves at 600 K at nodes 312 and 322 for the space flight ampoules.[3]

SAMPLE PREPARATION FOR POST-MISSION ANALYSES

The sample numbers for each specimen used in both the ground base and space flight experiments are shown in Tables 6 and 7. After the completion of the melting experiments (both ground base and space flight) the samples were returned to the Oak Ridge National Laboratory (ORNL). After removal from the ampoules, specimens A and A-R were potted in araldite epoxy for sectioning longitudinally. Since the B specimens were contained in the mild steel ampoules which would be wet by the molten specimens, the ampoules were mounted in epoxy resin and the ampoules, together with the B specimens, were sectioned longitudinally. The epoxy potting material was then dissolved from samples and the samples together with seven Pb-Au calibration disks were then remounted in a 5-cm diam araldite epoxy mount and metallographically polished.

The samples were irradiated in the Bulk Shielding Reactor (BSR) at ORNL for 4 hr and 2 MW in essentially a pure thermal flux of 1.2×10^{12} neutrons/sec·cm^2 In the irradiation both ^{209}Pb and ^{198}Au are formed. The activity of interest is ^{198}Au which decays by the emission of 0.960 MeV beta particles with a half life of 64.8 hr. The ^{209}Pb formed during the irradiation is essentially nonexistent after approximately 24 hr since the thermal neutron cross section for forming ^{209}Pb from ^{208}Pb is low and the ^{209}Pb half life is only 3.3 hr. After the radioactive nuclides decayed for 24 to 30 hr, autoradiographs of the specimens were made.

Autoradiographs were made in complete darkness in the same darkroom in which the film was developed subsequent to exposure. The polished face of the mount was placed face down on Kodak Industrial Type "R" X-Ray film, an ultrafine grain, single emulsion film. Exposures were made for 8, 16, 32, 64, 128, and 256-min. durations. The film is sensitized by β^- emission from the Au in the Pb. Since the range of the 0.960 MeV β^- in Pb is approximately 0.36 mm, only the Au concentration in this layer thickness is determined.

Table 6. Sample Number, Container Type, Temperature Region and Pb - 0.05 at. Percent Au Location for Space Flight Specimens

Container Type	Temperature Region, Pb-Au Alloy Location and Sample Numbers	
	Hot Zone	Cold Zone
Graphite	* | 11-A	* | 21-A
Graphite	13 A-R | *	17 A-R | *
Mild Steel	* | 12-B	* | 21-B

*Pb - 0.05 at. percent Au.

Table 7. Sample Number, Container Type, Temperature Region and Pb - 0.05 at. Percent Au Location for Ground Base Specimens

Container Type	Temperature Region, Pb-Au Alloy Location and Sample Numbers	
	Hot Zone	Cold Zone
Graphite	* | 17-A	* | 14-A
Graphite	11 A-R | *	20 A-R | *
Mild Steel	* | 13-B	* | 15-B

*Pb - 0.05 at. percent Au.

GOLD CONCENTRATION DETERMINATION USING A MICROPHOTOMETER

The Au concentration in each of the six space flight and six
ground base specimens is determined by scanning the autoradiographs with
a Jarrell-Ash recording microphotometer. Standards of Pb-Au which have
0, 25, 50, 100 200, 300, and 400 at. ppm Au are used to calibrate the
microphotometer. As stated previously, the standards are mounted with
each specimen and thus are irradiated and autoradiographed at the same
time. The 0 Au standard is used to set the transmittance of the
microphotometer at 100 percent. Before scanning the sample, a calibration
curve relating transmittance to Au concentration is determined by scanning
the Pb-Au standards. Over approximately 80 percent of the range of the
microphotometer, a linear relationship between the light transmitted and
the darkness of the autoradiograph exists. By making many autoradio-
graphic exposures (8, 16, 32, 64, 128, and 256 min.), it is possible to
get an autoradiograph that will allow the region of interest to fall
within the linear range of the transmittance curve. Each autoradiograph
is scanned longitudinally in 1-mm segments. The area viewed by the
microphotometer at any given time is 0.0065 x 0.5 mm. To date, one
slice of each space flight and each ground base sample has been irradiated
and autoradiographs and microphotometer scans have been made. However,
it will be a few weeks before quantitative analysis of the data will be
complete. At this time it will be possible to make some general
observations about the Au concentration distribution in the samples.

OBSERVATIONS AND DISCUSSION

Type A and A-R Ground Base and Space Flight Specimens From the Hot End of the Multipurpose Electric Furnace

In the last progress report, exterior characteristics of Type A
ground base and space flight samples were discussed;[2] for continuity, a
brief description will also be included in this report.

The ground base sample (17-A) and the space flight sample (11-A)
which were located in the hot end of the multipurpose electric furnace

are shown in Figs. 6-8. A side view of the samples is shown in Fig. 6. Upon cooling, samples 17-A and 11-A solidified from the bottom to the top as shown in the figures. Characteristics to be noted are:

1. The original bond interface of the Pb-Au disks can still be discerned at the top of each specimen.

2. Cellular structure is evident in the top part of 11-A but is not visible on the ground base sample 17-A.

Figure 6. Photograph of the ground base test (17-A) and space flight (11-A) specimens from the hot position of the electric furnace. The samples solidified from the bottom to top in ampoules with nonwetting walls. The samples are approximately 1 cm in diameter.

13

3. The ground base specimen showed the expected sharp
   corners at its base, while the space flight
   specimen has rounded corners at each end of the
   ingot.

A top view of the two samples is shown in Fig. 7; again the cellular
structure is seen in the space flight sample. Evidence of a solidifica-
tion pipe can be seen at the top of the ground base specimen 17-A. The
bottom end of the two specimens is shown in Fig. 8; ripple marks on the
base of the ground base specimen were caused by the quartz spacer cloth.
The space flight sample has a rounded edge and no evidence of ripple
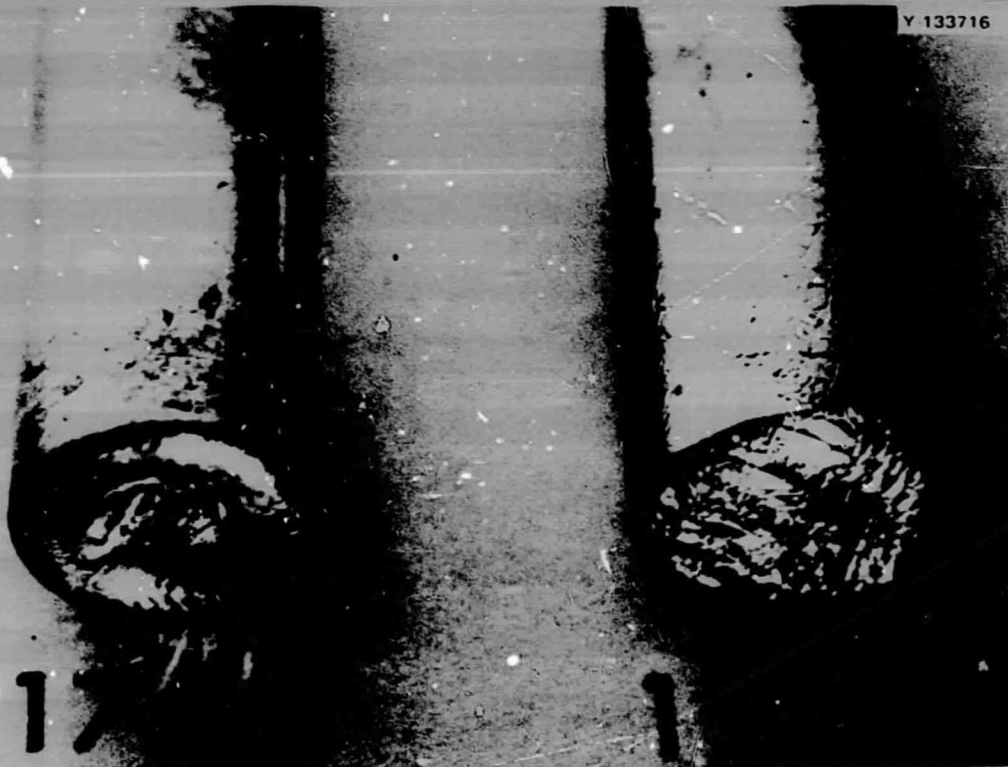marks from the quartz cloth.

Figure 7. Photograph of the top ends of the ground base test (17-A)
and space flight (11-A) specimens.

Figure 8. Photograph of the bottom ends of the ground base test (17-A) and space flight (11-A) specimens.

Side and bottom views of space flight sample 13 A-R and ground base sample 11 A-R are shown in Figs. 9 and 10, respectively. Recall that these samples are identical with samples 11-A and 17-A with the exception that the Pb-Au alloy is located on the opposite end of the specimens for the A-R samples. For the A-R samples the original Pb-Au alloy disk region melted last and solidified first. Characteristics similar to those noted for 11-A and 17-A are evident. Photographs for the Type B samples (contained in a wetting mild steel ampoule) from the hot end of the furnace were not obtained since they were not removed from their mild steel ampoules.

Y 134037

Figure 9. Photograph of the side view of ground base (11 A-R) and space flight (13 A-R) specimens from the hot zone of the electric furnace. The solidification direction is from the bottom to the top.

Figure 10. Photograph of the bottom sections of specimens 11 A-R and 13 A-R.

A print of an overexposed autoradiograph of space flight sample 11-A is shown in Fig. 11. The light areas represent Au activity and the seven Pb-Au standards (0, 25, 50, 100, 200, 300, 400 at. ppm Au) are shown beside the sample. The Au concentration in the central region of the original Pb-Au alloy disk which was located at the bottom of the sample is decreased from 500 at. ppm to approximately 125 at. ppm (Fig. 11). The Au concentration along the edges of the specimen in the vicinity of the original Pb-Au disk is decreased to approximately 90 at. ppm. Micro-photometer scans indicate that there is a small amount of Au (2-5 at. ppm) at the end of the sample; this is not evident from Fig. 11 but is

due to the fact the sample remained in the liquid phase for 268 min. which was much longer than expected. Note that the Au concentration profile is curved (concave with respect to the original Pb-Au disk).
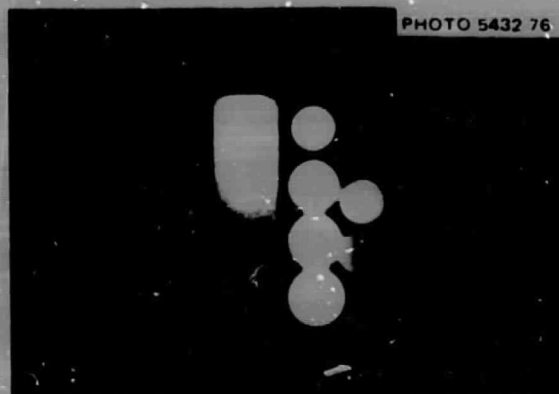

Figure 11. This is a print taken from an autoradiograph deliberately overexposed to emphasize the extent of Au diffusion in space flight sample 11-A. The light areas represent Au activity.

A print of an overexposed autoradiograph of ground base sample 17-A is shown in Fig. 12. The ground base samples were mounted vertically in the multipurpose electric furnace and thus sample 17-A (Fig. 12) melted from top to bottom and solidified from bottom to top. The solidification pipe can be seen at the top of the sample. As can be seen in Fig. 12, most of the Au has moved to the lower region of the sample. The microphotometer scans indicate that the Au concentration is approximately 30 at. ppm in the vicinity of the original Pb-Au alloy disk and approximately 75-80 at. ppm on the opposite end of the sample. The Pb-Au phase diagram predicts an equilibrium distribution coefficient during solidification of <1. Thus, if it is assumed that the Au was evenly distributed in the melt and the solidification front passed up the ingot, it would be expected that there would be a heavier concentration of Au near the top. It should be noted that since freezing occurred very rapidly, the effective distribution coefficient (K_{eff}) should be nearly equal to 1. Thus, solidification would have very little (if any) effect on the final Au concentration profile. The Au distribution shown in Fig. 12 cannot be explained by a solidification effect.

18

Figure 12. A print from an autoradiograph of ground base specimen 17-A.

Prints of autoradiographs of space flight sample 13 A-R and ground base sample 11 A-R are shown in Figs. 13 and 14, respectively. Recall that the A-R samples, like the A samples, were contained in nonwetting graphite lined ampoules; in the A-R samples the original Pb-Au alloy disk melted last and solidified first whereas the reverse was true for the A samples. As one might expect, the Au concentration for sample 13 A-R is similar to that for 11-A. The Au concentration is reduced to approximately 115-120 at. ppm in the central region of the original Pb-Au alloy disk and there are small amounts of Au (2-4 at. ppm) at the opposite end of the sample. The Au concentration at the edge of the original Pb-Au disk has reduced from 500 at. ppm to approximately 100 at. ppm. The cellular structu 'n the Au rich region of the sample can be seen. The curved Au concentration profile is not as evident in this case as it was with sample 11-A.

The Au concentration profile for ground base sample 11 A-R can be clearly seen in Fig. 14 as being convex with respect to the original Pb-Au alloy disk. In contrast with sample 17-A, most of the Au remained in the region of the original alloy disk. It should be recalled that in this sample the Pb-Au alloy disk was at the bottom of the sample. The
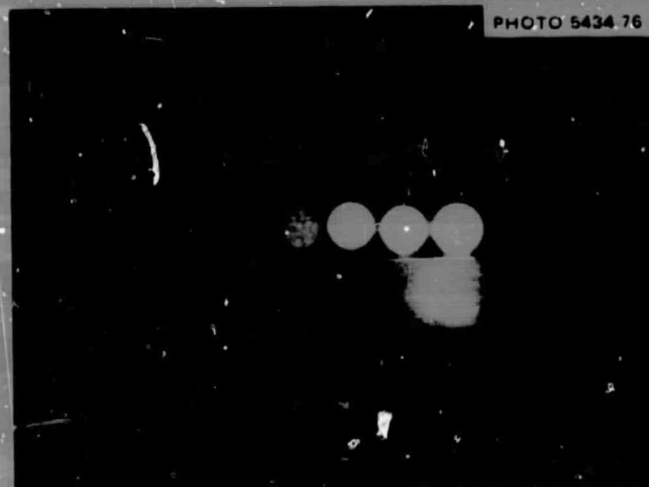
Figure 13. A print from an autoradiograph of space flight sample 13 A-R.

Figure 14. A print from an autoradiograph of ground base sample 11 A-R.

Au concentration at the bottom of the sample is reduced from 500 at. ppm
to approximately 160 at. ppm and on the opposite end it is approximately
5-10 at. ppm. One possible explanation for the Au distribution in
sample 17-A is that instabilities upon melting caused the Au to flow to
the bottom of the sample.

Prints of the autoradiographs of space flight sample 12-B and ground
base sample 13-B are shown in Figs. 15 and 16, respectively. These
samples were mounted and irradiated in their mild steel (wetting)
containers. (The hole in the Au-rich region of specimen 12-B could
possibly be due to shrinkage porosity.) The Au concentration in the
vicinity of the Pb-Au disk decreased to 85-90 at. ppm with 3-5 at. ppm
Au at the opposite end of the specimen. The ground base sample (13-B)
in Fig. 16 has an approximately uniform Au distribution across the sample
with an average concentration of Au of 35-40 at. ppm everywhere except at
the grain boundary where the concentration is much higher.

Figure 15. A print from an autoradiograph of space flight specimen
12-B. The wetted mild steel ampoule can be seen. The light areas in
the end caps do not represent Au activity, but other activities that are
the result of the thermal neutron irradiation of the mild steel ampoule.
The light area in the Pb does represent Au activity.

Figure 16. A print from an autoradiograph of ground base sample 13-B. Note the Au activity in the grain boundary. The Pb sample is fairly dark because the Au concentration is low and is fairly uniform over the sample.

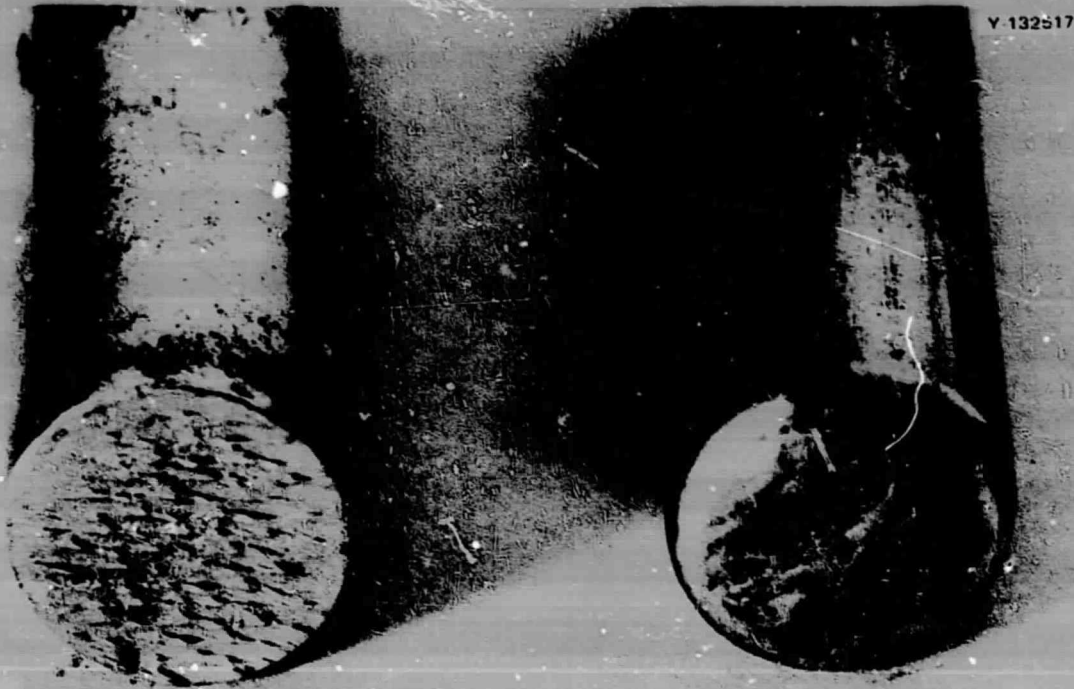## Ground Base and Space Flight Specimens From the Cold End of the Multi-purpose Electric Furnace

The exterior surfaces of A and A-R ground base and space flight samples which were located in the cold end of the electric furnace are shown in Figs. 17-21. Side views of space flight sample 21-A and ground base sample 14-A are shown in Fig. 17. As was noted with the hot zone samples, the original Pb-Au interface can be seen at the top of the samples. Cellular structure can be seen in the Pb-Au rich region of the space flight sample (21-A), but it is not evident in the ground base sample (14-A). The bottom ends of these two samples, shown in Fig. 18, have the same characteristics described for the hot zone samples 11-A and 17-A.

22

Y 132516

14-A   21-A

Figure 17. Photograph of the side view of ground base test (14-A)
and space flight (21-A) samples which were located in the cold zone of
the electric furnace. The samples solidified from the bottom to top in
ampoules with nonwetting walls.

14-A   21-A

Figure 18. Photograph of the bottom ends of ground base (14-A) and space flight (21-A) specimens.
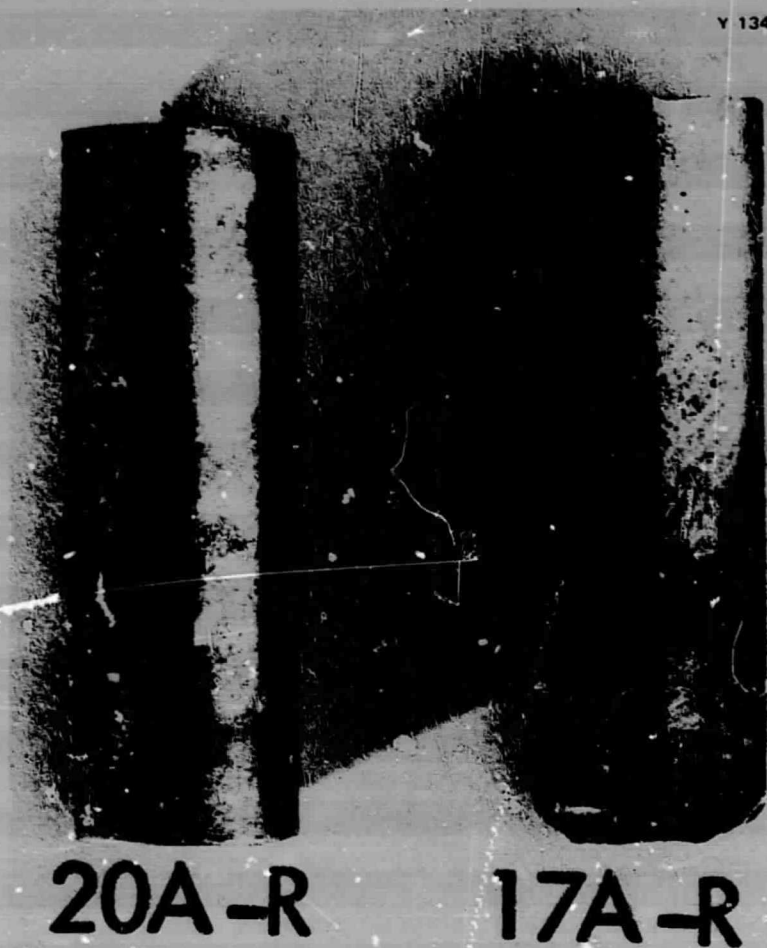
Y 134041

20A-R   17A-R

Figure 19. Photograph showing the side view of ground base (20 A-R) and space flight (17 A-R) specimens. The samples solidified from the bottom to the top.

Figure 20. Photograph of the bottom ends of specimens 20 A-R and 17 A-R.

Figure 21. Photograph showing the top view of ground base sample 20 A-R and space flight sample 17 A-R.

A side, bottom, and top view of samples 20 A-R and 17 A-R are shown in Figs. 19-21. Cellular structure in the space flight sample 17 A-R is not as evident as the hot zone space flight samples. Evidence of a large solidification pipe in space flight sample 17 A-R is seen in the top of the sample in Fig. 21.

A print made from an autoradiograph of space flight sample 21-A is shown in Fig. 22 which indicates the Au concentration profile to be curved. The microphotometer scans indicate a diffusion distance of 1.35 cm and that the Au concentration in the vicinity of the original Pb-Au alloy disk has dropped from 500 at. ppm to approximately 190-195 at. ppm at the center of the sample and to approximately 170 at. ppm at the edges.
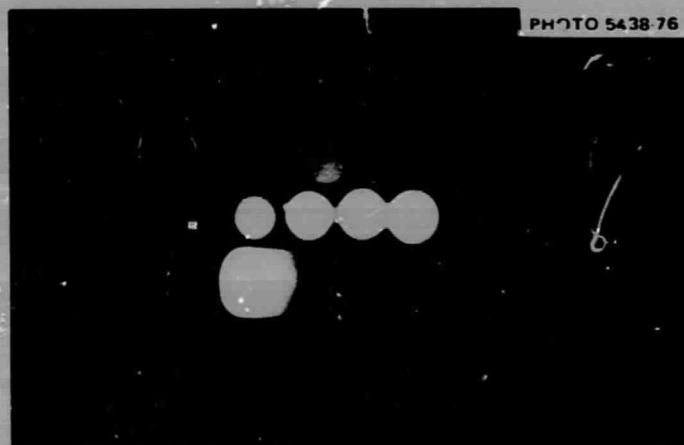

PHOTO 5438-76

Figure 22. A print of an autoradiograph of space flight sample 21-A. The light areas represent Au activity.

The Au concentration in the ground base specimen 14-A is shown in Fig. 23; as was true with the previous ground base specimen in the hot zone (17-A), most of the Au moved to the lower region of the specimen. In the figure, the original Pb-Au alloy was located at the top and the sample melted from the top and solidified from the bottom. The two elongated spots on the sample are lo areas caused by the metallographic polishing process. The Au concentration data for sample 14-A has been

obtained from the microphotometer scans and is shown in Table 8. The
sample was scanned longitudinally beginning at the top of Fig. 23, on
the side next to the standards. To avoid edge effects, the first and
last scan (Y_1 and Y_8) are approximately 1 mm from the edge of the
sample. Edge effects are caused by the asymmetric β^- scattering patterns
in those areas. The X values shown in Table 8 represent distances (mm)
along the sample cylindrical axis from the top to the bottom of the
sample as shown in Fig. 23. From Table 8 it is apparent that the Au
concentration in the area of the original Pb-Au alloy disk decreased to
approximately 27-30 at. ppm while the bottom end of the sample contains
60-70 at. ppm Au.

Figure 23. A print of an autoradiograph of ground base specimen
14-A.

The Au concentration data shown in Table 8 shows an asymmetric
variation across the diameter--concentrations being higher in the region
next to the standards. Since the asymmetric variation was seen for all
specimens, there is a high probability that the effect is due to β^-
particles originating from the Pb-Au standards. The magnitude of this

Table 8. Au Concentration (at. ppm) for Ground Base Sample 14-A - Cold Zone

X = Longitudinal distance along sample (mm).
X = 0 corresponds to the end of the sample where the original
    Pb-Au alloy disk was located.
Y_1 to Y_8 are radial distances across the sample (mm).
The Y values represent the central point of a 0.5 mm wide scan.

X	Y_1 = 1.25	Y_2 = 2.25	Y_3 = 3.25	Y_4 = 4.25	Y_5 = 5.25	Y_6 = 6.25	Y_7 = 7.25	Y_8 = 8.25
0.0	18	7	10	18	13	13	8	3
1.5	27	27	27	27	27	23	24	15
3.0	33	31	30	27	27	27	25	17
4.5	35	31	31	28	28	24	25	13
6.0	35	27	33	29	29	29	25	17
7.5	35	16	33	31	31	27	25	16
9.0	35	35	35	32	31	22	22	18
10.5	36	42	36	35	38	23	27	18
12.0	46	48	42	39	35	28	33	23
13.5	58	57	52	45	40	44	44	32
15.0	67	67	61	54	46	50	50	33
16.5	68	67	63	58	50	54	51	35
18.0	67	67	64	53	55	54	52	34
19.5	68	67	64	53	57	56	53	33
21.0	70	68	64	60	58	57	53	33
22.5	72	69	60	59	60	59	55	37
24.0	73	70	62	64	62	60	55	39
25.5	71	67	66	67	63	60	55	40
27.0	70	63	66	67	63	61	53	40
28.5	70	62	63	48	50	56	44	34
30.0	20	14	13	13	13	10	8	4

29

effect can be determined by rerunning a specimen which has been separated from the standards. This will enable corrections to be made for all specimens.

Prints of overexposed autoradiographs of space flight sample 17 A-R and ground base sample 20 A-R are shown in Fig. 24 and Fig. 25, respectively. Microphotometer scans indicate that the Au concentration for sample 17 A-R is similar to sample 21-A. In the central region of the original Pb-Au alloy the Au concentration decreased to 200-205 at. ppm and the Au diffusion distance is approximately 1.35 cm. The curved Au concentration profile is not as predominant for sample 17 A-R as it is for sample 21-A.

Ground base sample 20 A-R, shown in Fig. 25, indicates that once again the Au originally located at the bottom of the sample stayed at the bottom. The Au concentration decreased to approximately 200 at. ppm at the bottom whereas approximately 1-5 at. ppm is found at the opposite end.

Figure 24. A print of an autoradiograph of space flight sample 17 A-R.

Figure 25. A print of an autoradiograph of ground base specimen
20 A-R.

Prints of the autoradiographs for the Type B samples from the cold
zone of the furnace are presented in Fig. 26 and Fig. 27, respectively,
showing the Au concentration for space flight sample 21-B, Fig. 26, to
be similar to that for samples 21-A and 17 A-R; however, the Au appears
to have diffused slightly further into the sample. Diffusion distance
in sample 21-B was approximately 1.7 cm as compared with 1.35 cm for
space flight samples 21-A and 17 A-R which were also located in the cold
zone of the multipurpose furnace. The sample appears to have wet the
end of the mild steel ampoule that was adjacent to the original Pb-Au
alloy disk. The Au concentration profile is curved.

Most of the Au in ground base sample 15-B has moved from the area
of the 0.3 mm Pb-Au alloy disk to the opposite end of the specimen as
shown in Fig. 27. This behavior is opposite to that observed for
sample 13-B, the ground base sample contained in a wetting mild steel
ampoule located in the hot zone of the furnace, but it is identical to
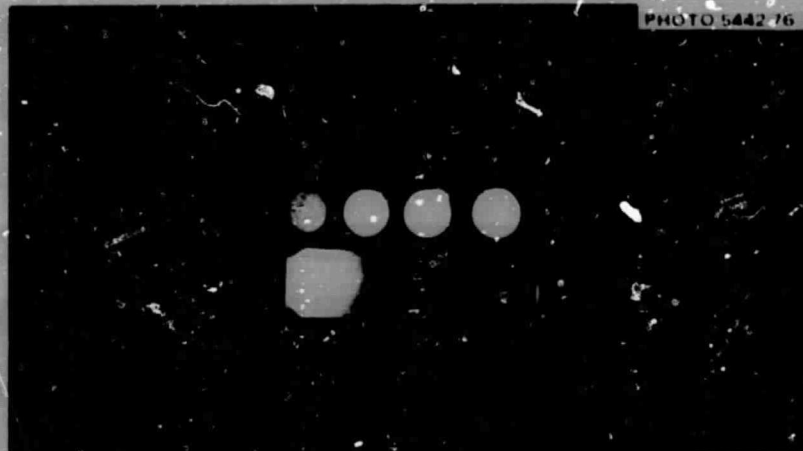what happened in ground base samples 17-A and 14-A which were contained

Figure 26. A print of an autoradiograph of space flight sample 21-B.

Figure 27. A print of an autoradiograph of ground base sample 15-B.

in nonwetting graphite lined ampoules and were located in the hot and cold zones of the furnace, respectively. The Au concentration in the vicinity of the original Pb-Au alloy disk has decreased to approximately 20 at. ppm while it has increased to approximately 65-70 at. ppm on the opposite end of the sample.

SUMMARY OF PRELIMINARY RESULTS

Space Flight Samples

(Refer to Table 6 for sample number, container type, temperature region, and original Pb-Au alloy disk location.)

1. The Au concentration distributions in space flight samples A and A-R (11-A and 13 A-R) from the hot end of the multipurpose electric furnace are similar. Microphotometer scans indicate that Au has traveled throughout the samples. The Au concentration value in the area of the initial location of the Au-Pb disk for space flight specimen 12-B decreased to a lower value than was observed for samples 11-A and 13 A-R. Again gold was distributed throughout the sample. Gold concentration profiles were curved for the A and B specimens, but the curvature was not as evident for the A-R specimen. Cellular structure was evident in the Au rich regions of samples A and A-R.

2. The space flight samples melted in the cold zone (723 K) of the furnace possess similar characteristics to those described in Result 1. Gold concentrations in samples 21-A and 17 A-R were similar and the diffusion distances were equal to approximately 1.35 cm. Although the initial Au concentration for 21-B was similar to 21-A and 17 A-R, the diffusion distance was approximately 1.7 cm. The Au concentration profiles are curved for samples 21-A and 21-B but again the curvature is not as evident for the A-R specimen (17 A-R). Cellular structure was noted in the Au-rich regions of the A and A-R specimens.

Ground Base Samples

(Refer to Table 7 for sample number, container type, temperature region and original Pb-Au alloy disk location.)

The Au concentration distribution in all ground base samples, with one exception, showed similar form, i.e., most of the Au that either started at the top or bottom of the specimen was found in the lower region of the sample. The one exception was sample 13-B wherein the Au was uniformly distributed except at the grain boundary in the lower region of the sample.

CONCLUSIONS

Determinations of Au distribution in each sample is not complete at this time; however, the following conclusions can be made:

1. The higher Au concentrations in the center of the specimens compared to the edges indicate that perhaps there is a small convection effect. Further investigations of this effect will be made.

2. The curved concentration profiles in the space flight samples have been observed in other experiments:

   a. Zinc self-diffusion experiment aboard Skylab.[5]
   b. Indium self-diffusion in unit gravity.[6]

   No explanation was given for the curvatures obtained in the zinc self-diffusion experiment; however, the indium results was explained by a wall effect.

3. Space-flight samples exhibited cellular structure in the Au-rich regions.

4. It appears there is no solidification effect on the diffusion profiles obtained for the space flight samples.

5. At present there is no explanation other than a
general assumption of instabilities upon melting
to account for the Au concentration in the ground
base specimens. With one exception (13-B) most of
the Au that started at the top of the specimen or
at the bottom of the specimen either moved or
stayed at the bottom.

ACKNOWLEDGMENTS

REFERENCES

1. Reed, R. E., Progress Report of Apollo—Soyuz Test Project Experiment No. MA-041 for the Period September 1-December 31, 1974, ORNL TM-4812, April 1, 1975.

2. Reed, R. E., Progress Report of Apollo—Soyuz Test Project Experiment No. MA-041 for the Period August 4-October 10, 1975.

3. Key, W. S., Technical Letter ASD-EP44-22716, Teledyne Brown Engineering, December 16, 1975.

4. Passaglia, E., National Bureau of Standards, Personal Communication.

5. Braski, D. N., Kobisk, E. H., O'Donnell, F. R., "Preparation, Testing and Analysis of Zinc Diffusion Samples," NASA Skylab Experiment M-558, ORNL-4956.

6. Nachtrieb, N. H., Self-Diffusion in Liquid Metals, The Properties of Liquid Metals, Edited by Adams, Davies and Epstein, September 1966, p. 313.